SSRG International Journal of Mechanical Engineering
ISSN: 2348-8360/ https://doi.org/10.14445/23488360/IJME-V13I4P103

Volume 13 Issue 4, 28-38, April 2026
© 2026 Seventh Sense Research Group®

Original Article

Design and Modelling of Pipe Climbing Robot (PCR) using Coppeliasim and Ensuring its Stability using Edge Impulse Software

Rakesh Rajendran[1], Hamsadhwani Vivekanandan[2], Meena.K[3], Karthick.M[4], Shivakumar Natarajan[5], Maghesh Kumar. D[6]

[1]*Department of ECE, Periyar Maniammai Institute of Science and Technology, Tamil Nadu, India.*
[2]*Department of EEE, Periyar Maniammai Institute of Science and Technology, Tamil Nadu, India.*
[3]*Department of CSE, Periyar Maniammai Institute of Science and Technology, Tamil Nadu, India.*
[4]*Department of Education, Periyar Maniammai Institute of Science and Technology, Tamil Nadu, India.*
[5]*Department of Mechanical Engineering, Periyar Maniammai Institute of Science and Technology, Tamil Nadu, India.*
[6]*Department of Computer Science, Periyar Maniammai Institute of Science and Technology, Tamil Nadu, India.*

[1]*Corresponding Author : rak2win@gmail.com*

Received: 06 January 2026 Revised: 12 February 2026 Accepted: 15 March 2026 Published: 29 April 2026

Abstract *- The oil and gas pipes in ships and marine oil refineries are prone to rapid corrosion.The leakage of these pipelines either occurs naturally or artificially due to man-made errors during usage. Hence, it is mandatory to have continuous monitoring over the entire pipeline systems by performing non–destructive testing NDT randomly. To perform these NDT, nowadays manual operations are being replaced with robotics and automation. There are many researchers who have developed their own designs for pipe leakage monitoring robots. Some robots travel inside the pipeline to detect interior leakage, whereas other types of robots climb the exterior of the pipe and investigate the outer layer. In this article, one such exterior pipe climbing robot named T-Bot is introduced, which can climb the parallel pipes with varied adjustable lengths, which remains the novelty of the proposed design. The design was initially modelled in simulation software named Coppelaisim, and then the payload capacity was tested and verified with an actual fabricated one in a lab test. The static and dynamic performance of the proposed T-Bot design is studied with respect to the payload-to-weight ratio (p: w) in both simulation and real-time testing. Another software named FEMM is utilized to validate the design with respect to magnetic flux lines. Finally, an attempt is made to study the stability of the T-Bot using the Internet of Things concept via the Edge impulse platform.*

Keywords *- NDT, T-Bot, Pipe Climbing Robot, Edge impulse, Anomaly detection.*

1. Introduction

The maintenance of pipelines in oil and gas refineries remains a big challenge, especially when these refineries are on the ocean. As the possibility of pipes getting corroded is higher in sea regions, the periodic maintenance of these pipes, done manually, remains a risky and challenging task. Many researchers have contributed to the design and fabrication of these pipe-inspecting robots. These pipes need to be tested both interior and exterior via visual inspection and nondestructive testing. The payload capacity, self-weight, and compatibility remain as vital features in deciding the performance of these inspecting robots used for pipe inspection. In this article, the proposed pipe inspection robot named T-Bot has the potential to navigate on the surface of three pipes at the same time, and hence, the time taken for scanning will be reduced when parallel pipes are considered. Bhadoriya et al [1] proposed an in-pipe inspection robot using a DC motor, which can be used for narrow pipes. In this work, the horizontal and vertical configuration of the pipe was plotted in a simulation. John et al [2] proposed an in-depth review of existing in-pipe inspection robots and discussed in detail the criteria for selection of a certain robot based on the specified criteria. Mthimkhulu et al [3] proposed an in-pipe inspection robot to detect the leakage area using the image processing technique. Sugin Elankavi et al [4] proposed a detailed review of the wheeled type in pipe inspection robots and found the research gaps in its design while comparing the existing pipe inspection robots. Li et al [5] introduced a novel design for an oil pipe inspection robot focusing on 6 design features that emphasize overcoming obstacle challenges. Chaojie Xu et al [6] proposed a study that examines the concepts, tasks, and application scenarios of various robot types, classifies and contrasts pipeline robots from various angles, and evaluates how adaptable they are in oil and gas

This is an open access article under the CC BY-NC-ND license (http://creativecommons.org/licenses/by-nc-nd/4.0/)

pipeline environments. It specifically enumerates the main technologies of the pipeline robot. Jeon et al [7] proposed an in-pipe inspection robot. consisting of a front and rear drive section, consisting of 22 motors. To keep an eye on the pipeline's inside, the robot has cameras and Lidars on both the front and back. Ogai et al [8] discussed an extensive network for pipelines engaged for various transportation purposes. Chen et al [9] discussed the technical limitations of the current pipeline monitoring system, inspection, and fitness for service, with key research areas focusing on pipeline body inspection. Sugin Elankavi et al [10] discussed in detail the design and development of a two-wheeled in pipe inspection robot overcoming the limitations of existing pipe inspection robots. Jain et al [11] developed a scissor mechanism made of two cross links, and a lead screw is used in the innovative PIR design concept to self-adjust and manage the robot while it is in motion. A DC motor regulates the scissor mechanism's motion. The kinematics and dynamics of the scissor mechanism will be justified with a mathematical model. A software named ADAMS is used for kinematics and dynamics simulation.

Table 1. Comparison of features of existing research on Pipe Climbing Robot

Research Article (Year)	Robot Type / Name	Locomotion Mechanism	Adhesion / Gripping Method	Key Features	Performance Highlights	Limitations
Gokul et al.[33] (2021)	Wheeled External Pipe Climber	DC motor-driven wheels	Spring-loaded clamping	Simple design, remote-controlled operation, suitable for hazardous environments	Can move vertically & horizontally for inspection	Limited adaptability to bends and varying diameters
Dutta et al. [30] (2023) – Complibot	Compliant External Robot (Inchworm type)	Inchworm motion using lead screws	Bistable compliant gripper	Uses bistable beam mechanism, energy efficient gripping, Arduino-controlled	Load capacity: 114.64 N, velocity: 0.2 m/min, no slip in PVC pipes	Slow movement, complex mechanical design
Lin et al. [34] (2026) – SMART-PIPEBOT	Soft External Pipe Robot	Soft pneumatic crawling	Vacuum suction + tail support	Bio-inspired (woodpecker tail), single-sidewall adhesion, flexible body	Vertical speed: 12.63 mm/s, works on wet surfaces, improved payload positioning	Lower speed, limited payload capacity
Reconfigurable Robot Study Inbar et al [35] (2022)	Reconfigurable External/Hybrid Robot (RSTAR-like)	Wheeled + adjustable geometry	Friction-based side force	Adjustable width, COM shifting, autonomous climbing strategies	Speed: up to 25 cm/s (vertical), adapts to 12–33 cm pipes	Complex control and mechanical system
Review Paper[36] (2023)	Multiple External Designs (Review)	Wheels, tracks, legged, hybrid	Friction, magnetic, suction	Summarizes propulsion, steering, localization methods	Identifies best mechanisms for inspection & maintenance	No specific prototype, general study
Proposed PCR	T-Bot external PCR	Arm type with adjustable length	Friction, magnetic, suction	Uses T-Shaped arm which enhance stability and also adaptability	The p:w is 23.8 for the proposed bot	Lower speed, limited payload capacity

Yahya et al [12] developed a parallelogram wheeled leg robot, which has higher adaptability compared to other existing pipe inspection robots. Nayak et al [13] encountered the possible critical design challenges of existing pipe inspection robots and proposed a novel screw drive type mechanism with a wall-press-adaptable wheel. Yoon et al [14] proposed an innovative bioinspired inchworm-type pipe inspection robot having two ball joints and a clamping, expandable device with a non-electrical driving device. Akimbay et al [15] developed an in-pipe inspection robot for cleaning the debris inside the pipe; in addition to the primary functions, it also performs anomaly detection and inspection, in pipe maintenance, etc. Jayakumar et al [16] proposed a wireless robot for pipe inspection by means of collecting images and transmitting wirelessly, overcoming tough and challenging situations.

Chaojie Xu et al [17] have reviewed all existing pipe inspection robots used in complex infrastructure engaged in the global energy transportation network. Karkoub et al. [18] proposed a robotics system with CCD cameras and a conical mirror, enabling visual pre-scanning before using costly ultrasonic and magnetic probes for testing or inspection. Patel et al [19] proposed a multi-robot system comprising two SWIM–R vehicles and one companion surface vehicle, which cleans the marine growth from the surface just before inspection. Khan et al [20] developed a custom vision-guided ultrasonic inspection tool enhanced with a graphical interface in a robotics work cell. The existing pipe climbing robot designs are lacking in adaptability to climb multiple pipes at the same time. Another important constraint lies with its payload capacity; the proposed T -Bot is an external pipe climbing robot with provision to adjust its T length in order to manage its payload capacity too. A novel pipe-cleaning robot was developed for an unknown workspace (21). A detailed review of existing pipe design and its application was presented (22). An in-pipe inspection robot enabled with IoT is presented (23). A material-driven pipeline inspection robot was developed (24). An AI-powered machine learning algorithm for defect identification and in-pipe navigation for pipe inspection robots was developed (25).

2. Methodology

The overall methodology is split up into four steps. In step I, it is assumed that there is no tangential force and only the normal force acts perpendicular to the surface in all 4 cases. In step II, the proposed T-shaped wall Climbing Robot is initially designed using the software FEMM to analyze its magnetic flux line distribution on the surface and to identify the pattern of magnetic flux intensity.

In step III, the proposed T-shaped Wall Climbing Robot is designed in a CoppeliaSim environment with two arms, A1 and A2. In step IV, the actual real-time testing is performed with the fabricated T Bot in the lab environment.

3. Step-1 Mathematical Analysis - T –Bot in Static Mode

The adhesive force exerted by the solenoid is denoted as Xi, and the required adhesive force is denoted as Fa^1, Fa^2, Fa^3, and Fa^4 for four different cases. The weight of the T bot is denoted as G. The value of G here is 420 grams or 0. 42kg. Case 1 considers the T-Bot on a vertical wall exactly perpendicular to the ground.

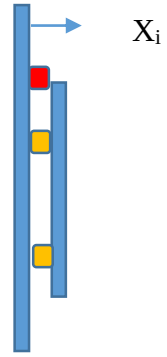

$$F_a^1 = \sum_{i=1}^{4} X_i \quad (1)$$

Fig. 1 T-Bot on vertical wall (Fa^1)

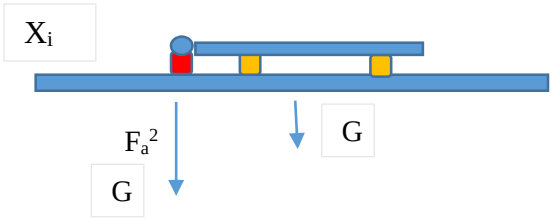

$$F_a^2 = \sum_{i=1}^{4} X_i - G \quad (2)$$

Fig. 2 T-Bot on vertical wall (Fa^2)

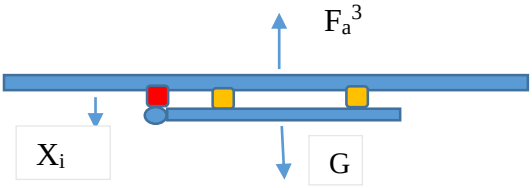

$$F_a^3 = G + \sum_{i=1}^{4} X_i \quad (3)$$

Fig. 3 T-Bot on vertical wall (Fa^3)

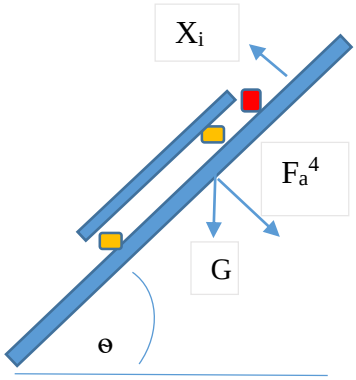

$$F_a^4 = \sum_{i=1}^{4} X_i - G\cos\theta \qquad (4)$$

Fig. 4 T-Bot on vertical wall (Fa^4)

Case 2 considers T Bot resting on horizontal ground. Case 3 is analyzed by considering the T-Bot in upside-down inverted position, sticking to the overhead metal wall. Case 4 is analyzed by considering the T-Bot on an inclined wall having an inclination of angle Ɵ.

Considering the angle of inclination as 45^0. The suction force exerted by solenoid Xi is considered to be 15 kg or 147 N. With these values of Xi and G and applying equations 1 to 4, the required adhesive force value Fa^1, Fa^2, Fa^3, and Fa^4 are obtained as shown in Table 2 below.

Table 2. Comparison of required adhesive force

Case num	Denotation	Required adhesive force (kgf)
Case-1	Fa^1	60
Case-2	Fa^2	59.58
Case-3	Fa^3	60.42
Case-4	Fa^4	59.71

4. FEMM Analysis

The proposed T-shaped wall Climbing Robot is initially designed with the software named FEMM to analyze its magnetic flux line distribution on the surface and also to identify the pattern of the flow of magnetic flux intensity.

Initially, the design is made in the FEMM platform by connecting nodes and internodes, then appropriate material and channel mediums are chosen, after which a mesh is created, and finally, the analysis is done. Figure 6 shows how the counters are declared in order to plot the graph.

Figure 7 shows the magnitude of flux density, having a value ranging between $8.9e^{02}$ and $9.4e^{02}$ tesla. The magnitude of the field intensity is found to reach the peak value four times exactly when the counter is passing through the solenoid location of the proposed T –Bot.

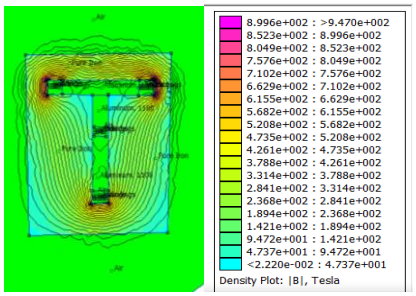

Fig. 5 T-Bot with magnetic flux density

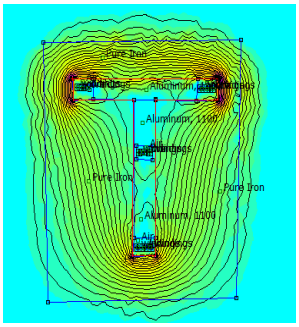

Fig. 6 T-Bot with counter established

Figure 8 depicts the variation of normal flux density along the surface of the proposed T-Bot. The magnetic field inside a long, current-carrying solenoid that is homogeneous and parallel to the central axis is referred to as the "normal field intensity." The magnetic field intensity at each point inside a perfect solenoid, which has tightly wrapped turns and is infinitely long, is constant in both magnitude and direction. Figure 9 shows the pattern of tangential flux density. The part of the magnetic flux density parallel to a surface boundary is called the tangential flux density.

Tangential flux is frequently reduced when designing solenoids for certain uses; comprehending and managing it is essential for a number of performance aspects. Figure 10 shows the magnitude of field intensity. There are four peaks shot when the counter is near the solenoid location along the surface of T-Bot. A solenoid's internal magnetic field is closely correlated with its current and number of turns per unit length. Performance is enhanced by a stronger magnetic field intensity because it applies more force. Figure 11 shows the normal field intensity.

Figure 12 shows the tangential field intensity. All these graphical analyses show that there is no interference between the magnetic flux lines of the solenoids positioned in the T – Bot. Analyzing all the figures from Figures 7 to 12, it shows that the proposed design T-bot is found to be exerting a uniform magnetic flux line with less interference and providing a reliable adhesive mechanism, overcoming the peel-off and rollover challenges that prevail in any wall-climbing or pipe-climbing robots.

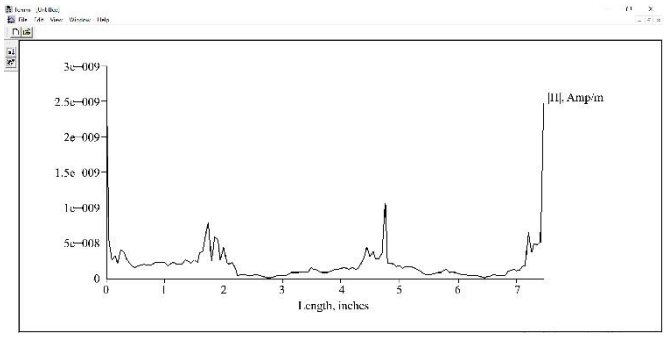

Fig. 7 Magnitude of flux density |B|

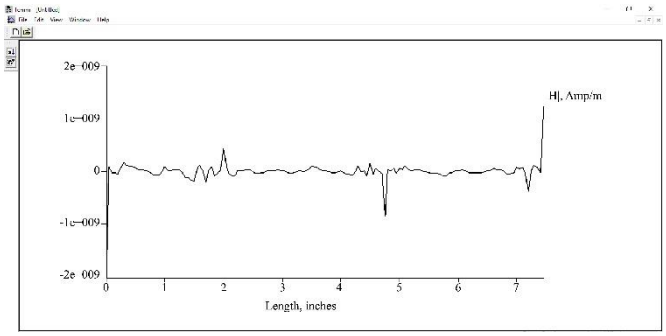

Fig. 8 Normal flux density B.n

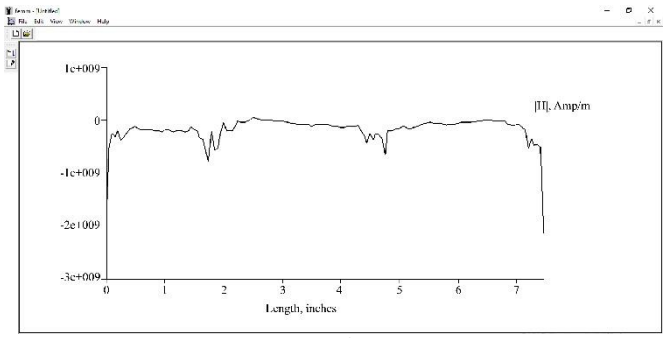

Fig. 9 Tangential flux density B.t

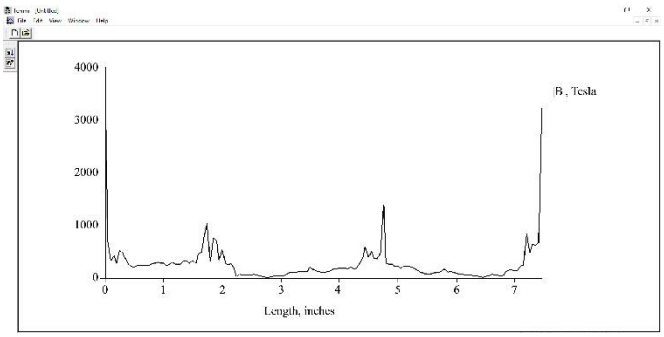

Fig. 10 Magnitude of field intensity |H|

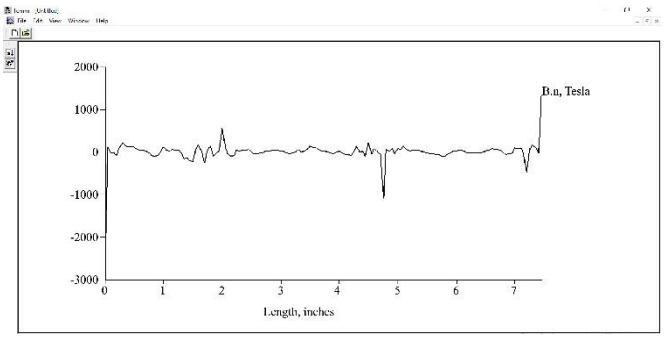

Fig. 11 Normal field intensity H.n

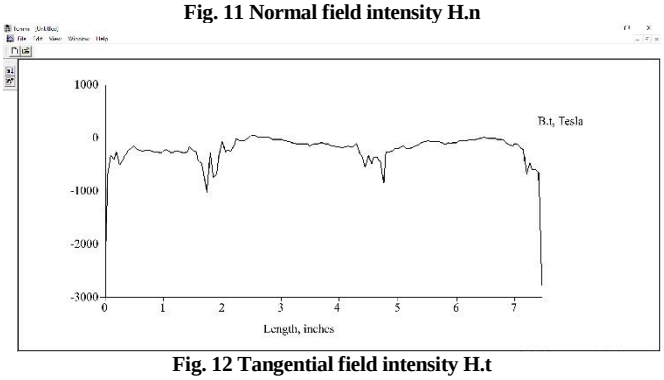

Fig. 12 Tangential field intensity H.t

5. Simulation Analysis – CoppeliaSim

The proposed T-shaped Wall Climbing Robot has two arms, A1 and A2, and is designed in a simulation environment named Coppeliasim. This software replicates the real-time environment, and hence, the trial and error process could be done for zero cost before actual fabrication. The proximity sensor is attached to the simulation model, replacing the solenoids in the real-time model.

The adhesive force of the sensor is considered to be 147 N (rounded to 150 N as shown in the figure), which is similar to the actual adhesive force value considered in a real-time experiment, i.e., 15 kg. The linear actuator is introduced at the junction of two arms, A1 and A2. In a simulation environment, the linear actuator is replaced with a prismatic joint.

The excitation of this proximity sensor is done in an alternating pattern so that T-Bot can either ascend or descend accordingly. The T-Bot can move only in uni direction, and hence the omnidirectional movement is not possible in this proposed design. The weight of the proposed T Bot is 0.42 kg and is fed into the simulation model. The time taken for ascending a defined height is noted in each trial and is tabulated as given in Tables 3 and 4.

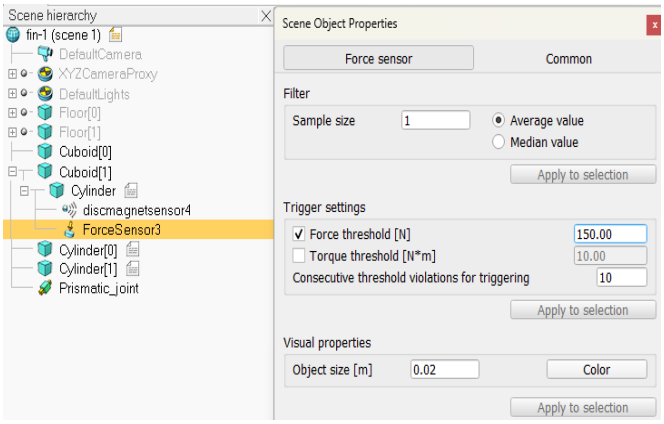

Fig. 13 Parameter feed in CoppeliaSim

The adhesive force of the proximity sensor can be fed as input through the Lua script. The payload capacity of the proposed T-Bot model can be studied both in dynamic and static modes, and this payload capacity of the T-Bot is varied via the parameter, as shown in Figure 13. This testing can be extended to n number of trials by varying the payload capacity and noting down the time taken to reach a particular height. The side view of the simulated model is shown in Figure 14, consisting of two Arms, A1 and A2, climbing over the metal wall. Figure 15 shows the front view of T-Bot, consisting of a prismatic joint between Arm 1 and Arm 2. The results obtained in the simulation are compared with those of the time taken during the real-time experiment, and these results are compared as shown in the graphs in Figures 20 and 21. The results say that the curve obtained with respect to payload and time taken in real-time experiment and simulation results are found to be in line with less deviation, and henceforth, this simulation tool would save time, effort, and waste obtained in the traditional trial and error method of modelling the design for wall climbing robots.

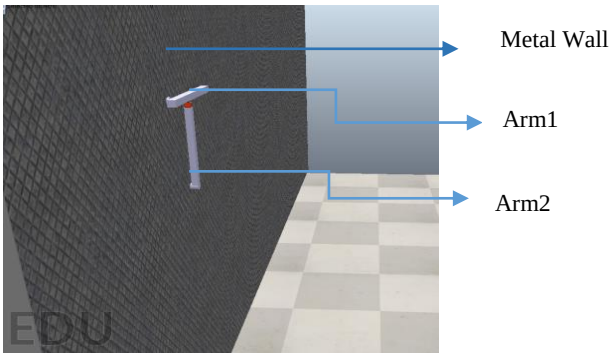

Fig. 14 T-Bot –side view of Simulated model in CoppeliaSim

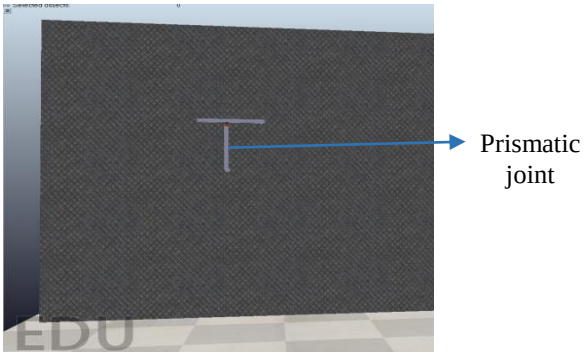

Fig. 15 T-Bot –front view of T-Bot with prismatic joint

6. Experimental Analysis – Hardware Testing

The proposed T Bot model, as simulated in Coppeliasim, is fabricated for performing the actual lab test. Figure 16 shows the front view of the T-Bot on the test wall. Figure 17 shows the side view of the T-Bot on the test wall. Figure 19 shows the T-Bot in static mode, carrying a 10 kg payload. Figure 18 shows the varied length of arm A2. The length varies from 15 cm to 20 cm. The length of the arm A2 can be varied manually with the probe and hole system. This feature is unique to the proposed Bot, making it adaptable to any gaps between the pipes. The arm A1 is connected with a DC motor, making it move forward and backward, which in turn makes the T–Bot climb up or descend down as a part of its navigation mechanism. Hence, the proposed model can only travel in uni direction and not in all directions. The actual weight of the T-Bot is found to be 0.42 kg, and the payload-to-weight ratio value (p: w) is found to be 23.81. The real-time lab test is further expanded to measure the time taken to reach a particular height (i.e., 10 cm) in the dynamic mode, and the result is tabulated as shown in the table. The T-Bot is further allowed to carry a varied payload ranging from 2 kg to 10 kg, and each time taken to reach a particular height is noted, and values are tabulated as shown in the table. Figure 20 shows the trend of the simulation results compared with the test results from an actual real-time experiment. The trend of the curve is found to be in line with the simulation results when compared with the real-time test experiment. The time taken for the T-Bot to climb the defined 20 cm is 1 minute 27 seconds.

Fig. 16 T-Bot –front view of T-Bot on Test wall

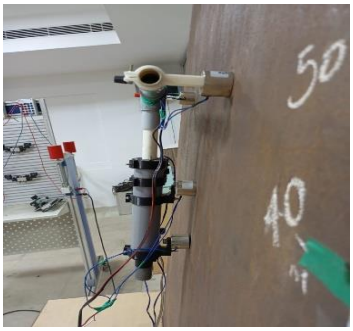

Fig. 17 T-Bot –side view of T-Bot on test wall

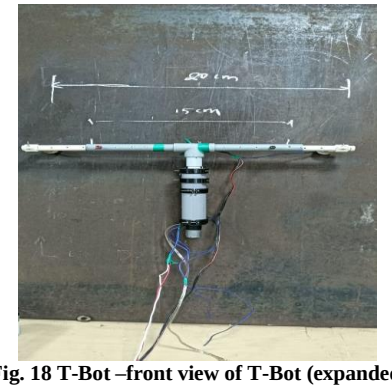

Fig. 18 T-Bot –front view of T-Bot (expanded)

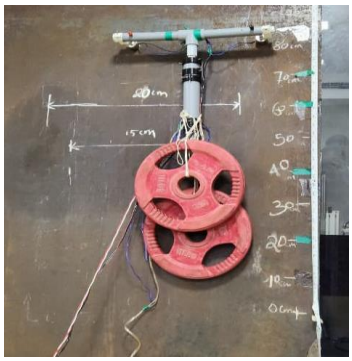

Fig. 19 T-Bot with payload 10 kg

Table 3. Height reached–simulation vs experimental

S.No	Time taken (min)	Simulation height reached (cm)	Experimental height reached (cm)
1	0	0	0
2	0.26	9	8
3	0.78	18	16
4	1.27	22	20

Table 4. Time taken - simulation vs experimental

S.No	Payload capacity	Height (cm)	Simulation time taken (s)	Experimental time taken (s)
1	2	10	70	75
2	4	10	80	95
3	6	10	100	110
4	8	10	120	130
5	10	10	145	150

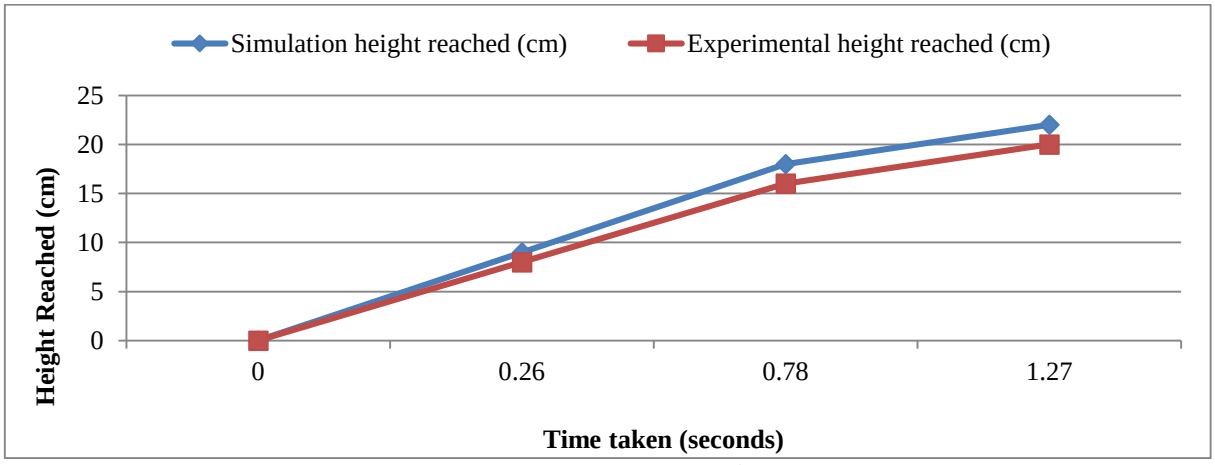

Fig. 20 T-Bot carrying a payload of 10 kg

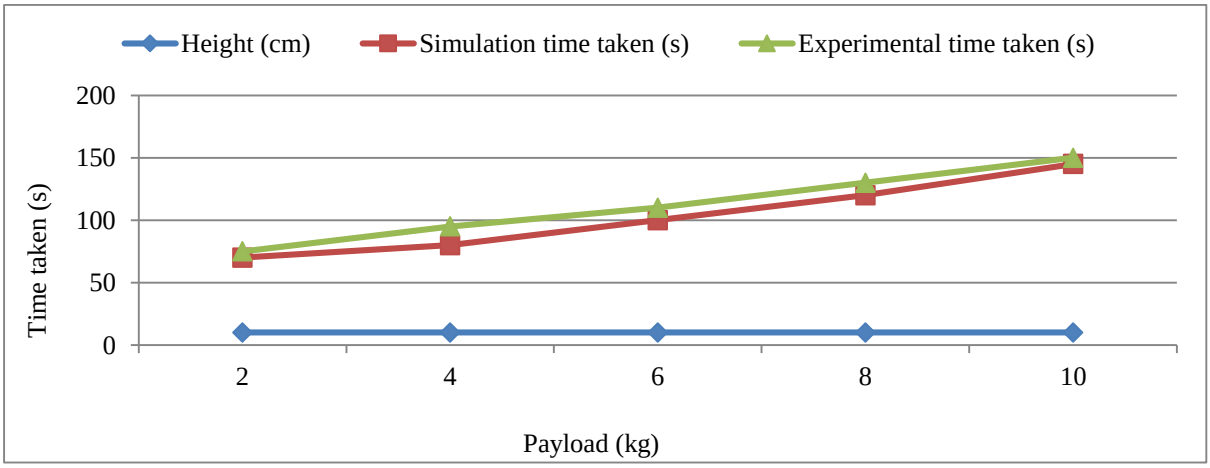

Fig. 21 Time taken Vs Height Reached

Table 5. Comparison of outcomes from FEMM simulation for Pipe Climbing Robot

Reference	|B| (T)	B·n (T)	B·t (T)	|H| (A/m)	H·n (A/m)
Zhang et al [26]	0.45	0.38	0.25	360	300
Li et al [27]	0.62	0.55	0.29	400	350
Le et al [28]	0.53	0.44	0.32	370	310
Shah et al [29]	0.57	0.48	0.35	390	340
Proposed T-Bot (PCR)	0.89	0.5	0.5	330	320

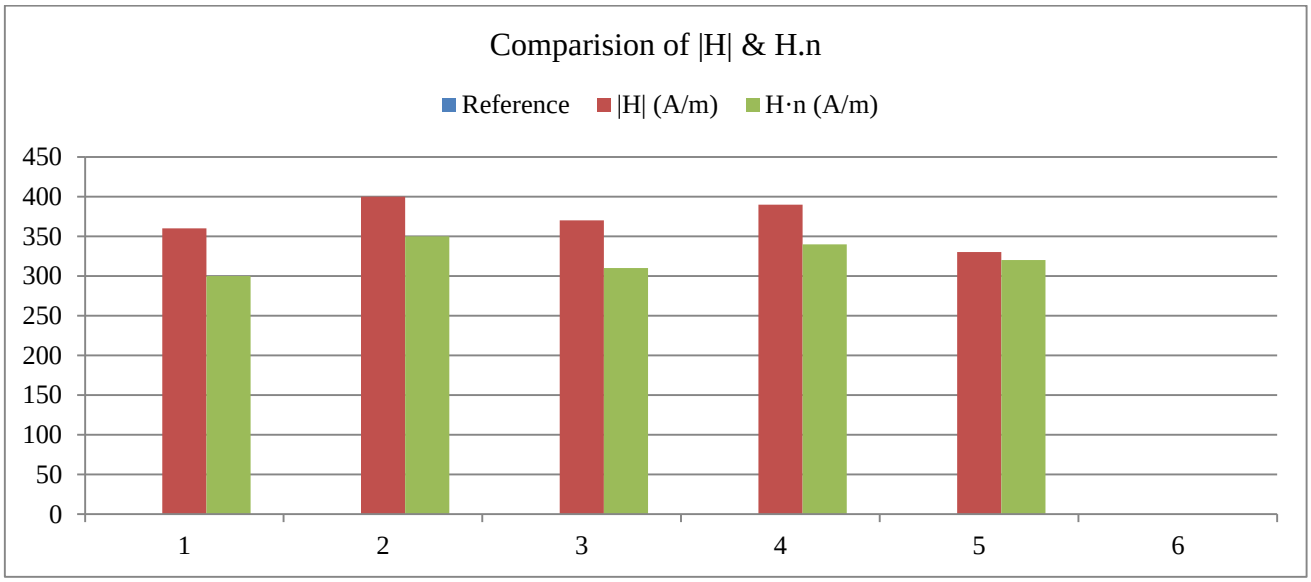

Fig. 22 Comparison of Magnetic field intensity

Edge impulse software is a unique platform where the data from sensors can be sent to the cloud, and machine learning models to predict and analyze the wave forms. Figure 22 shows the comparison of magnetic field intensity. The magnetic field intensity and magnetic strength vector value are almost the same in the proposed one, whereas they are variable in other work.

Table 6. Comparison of weight (w), payload (p), and p:w ratios of the existing Pipe Climbing Robot with the proposed T-Bot

Robot with reference	Weight (kg)	Payload (kg)	p:w ratio
Complibot (30)	Implied (≈22.5)	~11.7	0.52
Elastic Pipeline Robot (31)	(Not given explicitly)	30	–
Two-wheel Bite Robot (32)	~1.24 (implied from ratio)	11.4	9.16
T-Bot (Proposed bot)	0.42	10	23.81

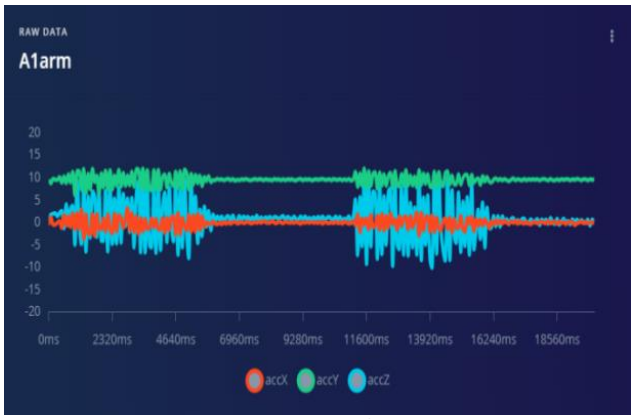

Fig. 23 Stability of Arm1

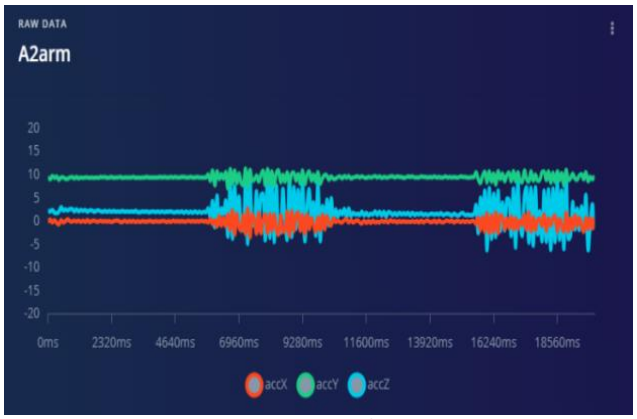

Fig. 24 Stability of Arm2

7. Discussion

Table 5 below shows the comparison of the magnitude of flux density |B|, Normal flux density B.n, Tangential flux density B.t, Magnitude of field intensity |H|, Normal field intensity H.n from the recent research articles with the proposed one. The proposed bot has a higher magnitude of flux density value when compared with existing research articles related to the pipe climbing robot. The parameter value shows that the proposed T-Bot exerts the value of other FEMM outcomes similar to the existing research article related to the pipe climbing robot. The above Table 6 shows the next comparison of the proposed T-bot pipe climbing robot with other existing research articles related to pipe climbing robots with respect to its self-weight, payload, and payload-to-weight ratio. The value shows that the proposed T-Bot pipe climbing robot exerts the highest value of p: w value in static mode (i.e., 23.81). It is also found that the proposed T-Bot is lighter (i.e., 0.4 kg) when compared to the self-weight of other existing pipe climbing robots.

8. Results

Figures 20 and 21 compare the test results obtained from the simulation results taken from CoppeliaSim and the results obtained from real-time hardware testing. In both graphs, it is clear that the simulation results and the real-time lab test results are in line with each other. The accelerometer and gyroscope sensors are coupled with Edge Impulse software to track the motion of Arm1 and Arm2 along the X, Y, and Z axes, thereby ensuring the stability of the proposed T-bot in dynamic mode, as shown in Figures 23 and 24. Figure 23 shows the stability of arm1, which ascends first while climbing. The graph shows there is more oscillation in the Z axis, which happens due to the wobbling effect of arm 1, which occurred as a result of the frictional movement of the solenoid (i.e., X_1 and X_2) on the rough surface of the cast iron metal wall or pipe. Figure 24 shows the stability of arm2, which ascends second, next to that of arm1. The Z axis is showing more oscillation when compared to the X and Y axes. Again, this oscillation or variation is due to the wobbling of solenoids (i.e., X_3 and X_4) along the Z axis. This vibration or oscillation occurred because of the frictional movement of the solenoids on the rough surface of the wall or pipe. Overall, the stability of the T-Bot is found to be good, as there is continuous movement occurring, overcoming the peel-off and rollover issues.

9. Conclusion

Thus, a pipe inspection robot or pipe climbing robot named T-Bot is designed with mathematical modeling in Step-I, by which a theoretical value of the desired or required adhesive force is obtained. This methodology ensures a paperwork calculation before arriving at the actual design of the proposed bot. The flow of the magnitude of flux density, normal flux density, tangential flux density, magnitude of field intensity, and normal field intensity and tangential field intensity are observed with FEMM simulation software for the proposed bot. The comparison of these values of the proposed T-Bot with the already existing pipe climbing robot is presented in Table 4. This kind of simulation analysis will ensure rectification of any further magnetic field interference while designing the proposed T-bot in Step-II. Another software named CoppeliaSim was used to model the design and perform the payload analysis, both in static and dynamic modes of the T-Bot over the metallic wall, which helped to ensure the fine-tuning of the design parameters before getting involved in actual fabrication. Here in Step-III, the time taken to reach a particular height with a varied payload and fixed payload capacity is tested in a simulation environment. Finally, in Step-IV, the actual T-Bot is fabricated with the obtained design parameters, and actual experimental tests within the lab are presented in this article for the proposed T-Bot. The proposed T-Bot is of self-weight 0.4 kg, and it has a payload lifting capacity of 10kg in static mode; hence, the payload-to-weight ratio obtained in this proposed T-Bot is 23.81, which is much higher than the other existing ones. Step IV also includes analyzing the dynamic stability of the T-Bot using the sensors integrated with Edge impulse software. The output from the accelerometer and gyroscope is read in X, Y, and Z axes, and the graph in Figures 23 and 24 shows the stability of arm1 and arm2 in the proposed T-Bot while climbing.

9.1. Limitations and Future Work

One limitation of this study lies with the standard deviation, peak amplitudes, or RMS vibration of the axis oscillations, which are not considered in this study, as the data from the Edge impulse platform is obtained only in the form of graphs. Another limitation is the measurement or estimation of the friction coefficient; the influencing factors, like cargo, arm geometry, motor torque ripple, or unequal magnetic force, which may be additional factors influencing the vibration, need to be considered in future work. The real-time testing of the fabricated T-Bot is done in the laboratory environment without considering the actual field test environment, where various other external factors may influence the testing. This work may be considered as a limitation of the proposed work and can be enhanced in the future scope of this work. Dynamic stability analysis should also be considered in the future scope of this work.

Acknowledgment

The authors acknowledge the Edge impulse platform, without which the Internet of Things concept and machine learning model could not be verified and tested. The work is done in the Robotics lab, CETAT, PMIST, with the facility capitalized by the seed money (Lr No.D.1282).

References

[1] Apoorv Vikram Singh Bhadoriya, Vijay Kumar Gupta, and Sujoy Mukherjee, "Development of In-pipe Inspection Robot," *Materials Today: Proceedings*, vol. 5, no. 9, pp. 20769-20776, 2018. [CrossRef] [Google Scholar] [Publisher Link]

[2] Binil John, and M. Shafeek, "Pipe Inspection Robots: A Review," *IOP Conference Series: Materials Science and Engineering*, vol. 1272, pp. 1-11, 2022. [CrossRef] [Google Scholar] [Publisher Link]

[3] Zinhle Mthimkhulu, Hannah Adebanjo, and Timothy T. Adeliyi, "Designing A Frugal Inspection Robot for Detecting In-Pipe Leaks in The Oil And Gas Sector," *2023 Conference on Information Communications Technology and Society (ICTAS)*, Durban, South Africa, pp. 1-6, 2023. [CrossRef] [Google Scholar] [Publisher Link]

[4] Rajendran Sugin Elankavi et al., "A Review on Wheeled Type in-Pipe Inspection Robot," *International Journal of Mechanical Engineering and Robotics Research*, vol. 11, no. 10, pp. 1-10, 2022. [CrossRef] [Google Scholar] [Publisher Link]

[5] Hui Li et al., "Development of a Pipeline Inspection Robot for the Standard Oil Pipeline of China National Petroleum Corporation," *Applied Sciences*, vol. 10, no. 8, pp. 1-15, 2020. [CrossRef] [Google Scholar] [Publisher Link]

[6] Chaojie Xu et al., "A Review: Research and Application of Pipeline Robots in the Oil and Gas Industry," *Journal of Pipeline Science and Engineering*, pp. 1-96, 2025. [CrossRef] [Google Scholar] [Publisher Link]

[7] Kwang-Woo Jeon et al., "Development of an in-Pipe Inspection Robot for Large-Diameter Water Pipes," *Sensors*, vol. 24, no. 11, pp. 1-20, 2024. [CrossRef] [Google Scholar] [Publisher Link]

[8] Harutoshi Ogai, and Bishakh Bhattacharya, *Pipe Inspection Robots for Gas and Oil Pipelines*, Pipe Inspection Robots for Structural Health and Condition Monitoring, pp. 13-44, 2017. [CrossRef] [Google Scholar] [Publisher Link]

[9] Pengchao Chen, "Advancements and Future Outlook of Safety Monitoring, Inspection and Assessment Technologies for Oil and Gas Pipeline Networks," *Journal of Pipeline Science and Engineering*, vol. 5, no. 4, pp. 1-10, 2025. [CrossRef] [Google Scholar] [Publisher Link]

[10] Rajendran Sugin Elankavi et al., "Design of a Wheeled-Type In-Pipe Inspection Robot to Overcome Motion Singularity in Curved Pipes," *Journal of Ambient Intelligence and Smart Environments*, vol. 16, no. 1, pp. 43-55, 2024. [CrossRef] [Google Scholar] [Publisher Link]

[11] R.K. Jain et al., "Experimental Performance of Robotic Inspection System for Underground Pipelines," *Journal of the Institution of Engineers (India): Series C*, vol. 102, pp. 683-703, 2021. [CrossRef] [Google Scholar] [Publisher Link]

[12] Nur Afiqah Binti Haji Yahya, Negin Ashrafi, and Ali Hussein Humod, "Development and Adaptability of in-Pipe Inspection Robots," *IOSR Journal of Mechanical and Civil Engineering*, vol. 11, no. 4, pp. 1-8, 2014. [CrossRef] [Google Scholar] [Publisher Link]

[13] Ankit Nayak, and S.K. Pradhan, "Design of a New in-Pipe Inspection Robot," *Procedia Engineering*, vol. 97, pp. 2081-2091, 2014. [CrossRef] [Google Scholar] [Publisher Link]

[14] Kyung-Hyun Yoon, and Young-Woo Park, "Pipe Inspection Robot Actuated by using Compressed Air," *2010 IEEE/ASME International Conference on Advanced Intelligent Mechatronics*, Montreal, QC, Canada, pp. 1345-1349, 2010. [CrossRef] [Google Scholar] [Publisher Link]

[15] Dias Akimbay et al., "A Novel Hybrid Robot for In-Pipe Maintenance and Inspection," *IEEE Access*, vol. 13, pp. 168498-168511, 2025. [CrossRef] [Google Scholar] [Publisher Link]

[16] D. Jayakumar, R. Jaganath, and R. Selvarasu, "Defect Identification in Pipelines Using Inspection Robot," *2016 Online International Conference on Green Engineering and Technologies (IC-GET)*, Coimbatore, India, pp. 1-5, 2016. [CrossRef] [Google Scholar] [Publisher Link]

[17] Rashmi Wijesundara et al., "Design and Simulation of a Soft Pipe-Climbing Robot for Scalable and Energy-Efficient Pipe Inspection Operations," *2025 IEEE 18th Dallas Circuits and Systems Conference (DCAS)*, Arlington, TX, USA, pp. 1-5, 2025. [CrossRef] [Google Scholar] [Publisher Link]

[18] Mansour Karkoub, Othmane Bouhali, and Ali Sheharyar, "Gas Pipeline Inspection using Autonomous Robots with Omni-Directional Cameras," *IEEE Sensors Journal*, vol. 21, no. 14, pp. 15544-15553, 2021. [CrossRef] [Google Scholar] [Publisher Link]

[19] Sahejad Patel et al., "Multi-robot System for Inspection of Underwater Pipelines in Shallow Waters," *International Journal of Intelligent Robotics and Applications*, vol. 8, pp. 14-38, 2024. [CrossRef] [Google Scholar] [Publisher Link]

[20] Aamir Khan et al., "Vision Guided Robotic Inspection for Parts in Manufacturing and Remanufacturing Industry," *Journal of Remanufacturing*, vol. 11, pp. 49-70, 2021. [CrossRef] [Google Scholar] [Publisher Link]

[21] Nguyen Truong-Thinh, Nguyen Ngoc-Phuong, and Tuong Phuoc-Tho, "A Study of Pipe-Cleaning and Inspection Robot," *2011 IEEE International Conference on Robotics and Biomimetics*, Karon Beach, Thailand, pp. 2593-2598, 2011. [CrossRef] [Google Scholar] [Publisher Link]

[22] Heesik Jang et al., "A Review: Technological Trends and Development Direction of Pipeline Robot Systems," *Journal of Intelligent & Robotic Systems*, vol. 105, 2022. [CrossRef] [Google Scholar] [Publisher Link]

[23] M.N. Mohammed et al., "A New Approach to Design and Development of In-Pipe Inspection Robots," *2024 Arab ICT Conference (AICTC)*, Manama, Bahrain, pp. 108-112, 2024. [CrossRef] [Google Scholar] [Publisher Link]

[24] Chao Tang et al., "A Pipeline Inspection Robot for Navigating Tubular Environments in the Sub-Centimeter Scale," *Science Robotics*, vol. 7, no. 66, 2022. [CrossRef] [Google Scholar] [Publisher Link]

[25] Darkhan Zholtayev et al., "Smart Pipe Inspection Robot with In-Chassis Motor Actuation Design and Integrated AI-Powered Defect Detection System," *IEEE Access*, vol. 12, pp. 119520-119534, 2024. [CrossRef] [Google Scholar] [Publisher Link]

[26] Heshan Zhang et al., "Analytical Prediction of Electromagnetic Performance for Surface-Embedded Permanent Magnet in-Wheel Machines Considering Iron's Nonlinearity," *Scientific Reports*, vol. 14, pp. 1-18, 2024. [CrossRef] [Google Scholar] [Publisher Link]

[27] Lian-bo Li, Tao Chen, and Wei-xuan Li, "Analysis of the Air Gap Magnetic Field in Cylindrical Magnetic Couplings based on Mathematical and Finite Element Approach," *Scientific Reports*, vol. 14, pp. 1-14, 2024. [CrossRef] [Google Scholar] [Publisher Link]

[28] Tan Nam Le et al., "Influence of Magnetic Fields on the Microstructure and Mechanical Properties of MIG Welds," *EAI Endorsed Transactions on Sustainable Manufacturing and Renewable Energy*, vol. 1, no. 1, pp. 1-6, 2024. [CrossRef] [Publisher Link]

[29] Janvi Shah et al., "A Hybrid Approach for Edge Detection using Fuzzy Logic and Canny Method," *International Journal of Engineering Research & Technology*, vol. 2, no. 3, pp. 1-6, 2013. [Google Scholar] [Publisher Link]

[30] Saurav Kumar Dutta, B. Sandeep Reddy, and Santosha Kumar Dwivedy, "Complibot: A Compliant External Pipe Climbing Robot," *Mechanics Based Design of Structures and Machines*, vol. 52, no. 4, pp. 2106-2135, 2024. [CrossRef] [Google Scholar] [Publisher Link]

[31] Jie Li et al., "Elastic Obstacle-Surmounting Pipeline-Climbing Robot with Composite Wheels," *Machines*, vol. 10, no. 10, pp. 1-17, 2022. [CrossRef] [Google Scholar] [Publisher Link]

[32] Rui Li et al., "A Two-Wheel Bite Embracing Modular Climbing Robot with High Load," *International Journal of Mechanical Sciences*, vol. 309, 2026. [CrossRef] [Google Scholar] [Publisher Link]

[33] S. Gokul et al, "Modern Literature Overview on Fabrication of External Pipe Climbing Robot," *International Journal of Research in Engineering, Science and Management*, vol. 4, no. 4, pp. 1-4, 2021. [Publisher Link]

[34] Sheng Lin et al., "SMART-PIPEBOT: A Soft Pipe-Climbing Robot with Woodpecker Tail-Inspired Support Mechanism for Single-Sidewall Adhesion," *Biomimetic Intelligence and Robotics*, pp. 1-18, 2026. [CrossRef] [Google Scholar] [Publisher Link]

[35] Ori Inbar, and David Zarrouk, "Analysis of Climbing in Circular and Rectangular Pipes with a Reconfigurable Sprawling Robot," *Mechanism and Machine Theory*, vol. 173, pp. 1-16, 2022. [CrossRef] [Google Scholar] [Publisher Link]

[36] Jalal Taheri Kahnamouei, and Mehrdad Moallem, "A Comprehensive Review of in-Pipe Robots," *Ocean Engineering*, vol. 277, 2023. [CrossRef] [Google Scholar] [Publisher Link]